A quantitative analysis of three-dimensional contact guidance by breast cancer cells

by
Emma A. Krnacik

A PROJECT

submitted to

Oregon State University

University Honors College

in partial fulfillment of
the requirements for the
degree of

Honors Baccalaureate of Science in Biochemistry and Biophysics
(Honors Scholar)

Presented May 28, 2015
Commencement June 2015

AN ABSTRACT OF THE THESIS OF

Emma A. Krnacik for the degree of Honors Baccalaureate of Science in Biochemistry and Biophysics presented on May 28, 2015. Title: A quantitative analysis on three-dimensional contact guidance by breast cancer cells.

Abstract approved:

_____

Bo Sun

Exploring and quantifying the parameters regarding contact guidance may provide valuable insight to the precise mechanisms controlling cell movement, especially in a three-dimensional environment. The objective of this project was to quantify the relationship between MDA-MB-231 cell morphogenesis and the geometry of the cell's local microenvironment, which was modeled by collagen networks of varying degrees of organization. Specifically, a non-linear correlation was found between the aspect ratio of the cell and the misalignment angle between average cellular and local fiber direction. This relationship was modeled by a power law function, which is proposed to be indicative of a cellular feedback mechanism between morphogenesis in MDA-MB-231 cells and fiber organization. Furthermore, using confocal immunofluorescence imaging the presence of proteins known to be critically involved in mechanosensing (specifically, actin and vinculin) was observed in cells exhibiting contact guidance in a three-dimensional network, suggesting molecular similarities in the processes of mechanosensing and geometry sensing.

Key Words: mechanosensing, contact guidance, polarization

Corresponding e-mail address: krnacike@gmail.com

©Copyright by Emma A. Krnacik
May 28, 2015
All Rights Reserved

A quantitative analysis of three-dimensional contact guidance by breast cancer cells

by
Emma A. Krnacik

A PROJECT

submitted to

Oregon State University

University Honors College

in partial fulfillment of
the requirements for the
degree of

Honors Baccalaureate of Science in Biochemistry and Biophysics
(Honors Scholar)

Presented May 28, 2015
Commencement June 2015

Honors Baccalaureate of Science in Biochemistry and Biophysics project of Emma A. Krnacik presented on May 28, 2015.

APPROVED:

_____

Bo Sun, Mentor, representing Physics

_____

David McIntyre, Committee Member, representing Physics

_____

Chris Jones, Committee Member, representing Physics

_____

Toni Doolen, Dean, University Honors College

I understand that my project will become part of the permanent collection of Oregon State University, University Honors College. My signature below authorizes release of my project to any reader upon request.

_____

Emma A. Krnacik, Author

ACKNOWLEDGMENTS

I would like to thank my mentor Dr. Sun for his continuous advice and direction throughout this project and the rest of Dr. Sun's lab group for their support and sharing of their knowledge. I would also like to thank my parents for their encouragement and for instilling an interest in scientific endeavors from the beginning.

INTRODUCTION

Contact guidance:

In the development of tissues in living organisms, it is well known that cells respond to environmental cues to influence growth and migration. While there has been extensive research on the process of chemosensing (cell detection of chemical signals), mechanosensing (cell detection of physical stimuli) is a much less well-understood area of cell functioning. The cell's response to the geometric microenvironment is known as contact guidance. The ability to direct a cell's morphology and motion through geometrical factors of the cell's local environment has many applications in cancer metastasis and regenerative medicine. For example, it has been observed that disorganization of the components of the cornea (such as seen in scarring) results in a loss of transparency and therefore functionality in humans. Contact guidance has been utilized to develop corneal stroma tissue on pre-patterned films consisting of organized collagen fibers. Studies have shown that increased transparency can be achieved by growth of keratocytes on micropatterned scaffold, simulating more accurate topography of the surrounding tissue in the cornea[1].

Cell polarization:

The mechanisms underlying cell migration on a two-dimensional surface have been extensively researched. For migration to occur, polarization of the cell

must be established. Cell polarization can be defined by the presence of a leading end and a lagging end, as well as the repositioning of the Golgi and the microtubule-organizing center, which is regulated by Rho family GTPases[2]. The leading strand is composed of a protrusion produced by actin polymerization, which is directly controlled by one of two protien complexes, either Arp2/3 complex or two formins (mDia1 and mDia2). Arp2/3 primarily directs actin polymerization from existing filaments in a non-linear fashion, while mDia1 and mDia 2 direct linear extension. Both protiens are mediated through different signaling cascades[3]. For my thesis study, cell polarization was measured morphologically by cell aspect ratio, and molecularly by confocal immunofluorescent imaging of the spatial organization of actin and vinculin.

Contact guidance in a 3D environment:

There is evidence that the mechanisms and signaling processes behind cell migration differ between two-dimensional and three-dimensional environments[4]. However, this is not yet a well-understood process. It is useful to recreate micro or nanostructures found in organisms to analyze the interactions between the cell and its physical environment. Even on the nanoscale region, small features in the extracellular matrix have been shown to effect cell function *in vivo*[5]. Since two-dimensional surfaces are not often an accurate representation of cancer cell environment *in vivo*, studying cell contact guidance from a three-dimensional

perspective can provide a more realistic model of cell migration and morphogenesis, especially in regard to cancer metastasis.

Obstacles and knowledge gaps:

Although studying cellular mechanisms in a three-dimensional environment may serve as a more realistic model for many cancers, this can be somewhat difficult to control and account for additional variables in comparison to a two-dimensional experimental environment. In addition, there are less complicating factors in introducing and growing cells on a two-dimensional surface due to the increased accessibility to the cell's environment. Studying contact guidance in two dimensions is therefore more convenient and simplistic.

Another possible complicating factor in three-dimensional migration is the resistive force experienced in a three-dimensional environment (or gel) as opposed to on a flat surface. Studies have suggested that in a three-dimensional matrix the migrating cell itself also affects the surrounding matrix through "characteristic reorganization", suggesting that movement of the cell itself will cause local fiber alignment. Circumscribed fiber reorganization was said to be due to dynamic fiber traction, localized fiber disruption, and the release of surface cell determinants at the detachment sites. This creates a tube-like path, on which nearby cells would also follow. In respect to the mechanics of cellular migration in a three-dimensional collagen environment, it has been observed that polar

localization of binding integrins occurs at either end of the leading and tail end of the cell, consistent with the respective collagen fibrils[6].

To address these challenges in my study, cells were embedded into the collagen matrix at a low density to avoid cell-to-cell interactions. To reduce possible cell influence on fiber directionality, linearly aligned fiber networks were established as the gel was being created, to ensure that the cells themselves were not creating the observed linear fiber alignment. In addition, cells were imaged 4-36 hours after creation of the gel to reduce the time cells had to disrupt the environment.

MATERIALS AND METHODS

Creation of the PDMS channel for radial collagen fiber alignment:

In order to create radial alignment of the collagen fibers, a small device molded out of polydimethylsiloxan (PDMS) was placed on a 24x44 mm glass coverslip. A rectangular well was cut out of a PDMS mold measuring approximately 5 mm in height, 24 mm in width, 35mm in length with walls 7.5mm thick (Fig 1).

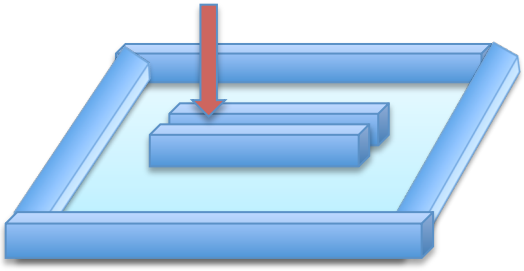

Figure 1: Depiction of the device used for radial alignment, with red arrow indicating the placement of collagen between the two channels. Image not to scale.

The purpose of the well surrounding the PDMS channel was to contain growth medium to preserve the cell-embedded collagen. Inside of the well, a channel 15 mm in length and approximately 2 mm in width was created by placement of two strips of PDMS, 0.5 cm in height and 2.5 mm in width in the center of the well. All PDMS pieces were adhered to the glass coverslip using a corona treater and left on a hot plate for one hour under a small weight to ensure a watertight seal between the surfaces. All devices were cleaned with ethanol before use.

Creating the cell-embedded collagen:

Type I rat tail high concentration collagen was used at a working concentration of 2 mg/mL. Polymerization of collagen fibers was initiated by the addition of 0.1 M sodium hydroxide and exposure to room temperature (21 ˚C). 10 μL of resuspended MDA cells in growth medium was added to a gel solution in a total volume of 200 μL. Polystyrene micro beads, 26.4 μm in diameter, were added to the solution at 0.01% of the total volume. Immediately after mixture of all components of the collagen gel, approximately 50 μL of solution was placed at the beginning of the PDMS channel. A radial force through the channel was induced through use of a spin coater.

Spin coating procedure:

Initial data was collected using a spin coating machine from Laurell Technologies, allowing the device to be spun at a constant speed for a set amount of time in order to create a radially directed force on the gel through the channel. The center of the spin circle was placed at the beginning of the channel, putting the end of the channel at the outer edge of the spin radius. Spin speed was set at 350 rpm and allowed to run for 10 minutes directly after creation of the gel.

After the spin coating process had completed, the gel was allowed to sit at room temperature for approximately 50 minutes for the solution to completely gelize. Growth medium was then added to preserve the sample, and it was placed in the incubator at 34 ˚C for 4-36 hours. This purpose of the wait time was to

allow the embedded cells to attach to the collagen environment and morphologically react in the presence of the new geometric microenvironment.

Cell-Tak procedure:

Ibidi microdishes were used for circular alignment and were pre-treated with Cell-Tak to adhere the collagen gel to the bottom of the glass dish. The dishes were 35 mm in diameter, with a well volume of 400 µL and a growth area of 3.5 cm^2. To prepare the Cell-Tak solution, 6 µL of Corning Cell-Tak (2.54 mg/mL) was combined with 30 µL of 0.1 M NaOH, 40 µL of PBS and 324 µL of DI water. The total volume of 400 µL was then pipetted into the Ibidi dish and allowed to incubate at 37 ˚C for 30 minutes. The dishes were then preserved at 4 ˚C until further use.

Circular collagen alignment procedure:

Circular alignment of collagen was used to achieve separate regions of higher and lower levels of collagen alignment (Fig 3). The goal of this was to not only quantify, but to control the degree of fiber alignment in order to more accurately determine a minimum threshold of necessary fiber alignment for influencing cell polarity. Collagen gel was created at a concentration of 2 mg/mL from type I high concentration rat-tail collagen at 11.00 mg/mL (see protocol for creating the cell-embedded collagen).

400 µL of 2 mg/mL collagen was added to fill the well volume of an Ibidi glass-bottomed dish and immediately taken for alignment. This was achieved using two needles approximately 4 mm apart, submerged in the gel. The needles were rotated at approximately 2.2 rpm for ten minutes after formation of the gel (Figure 2). For best results, the needles were slightly offset so that rotation occurred on two circular tracks, just offset from each other by less than 1 mm (as opposed to rotating on the same track, creating one perfect circle). The needles were removed and gel was allowed to incubate at room

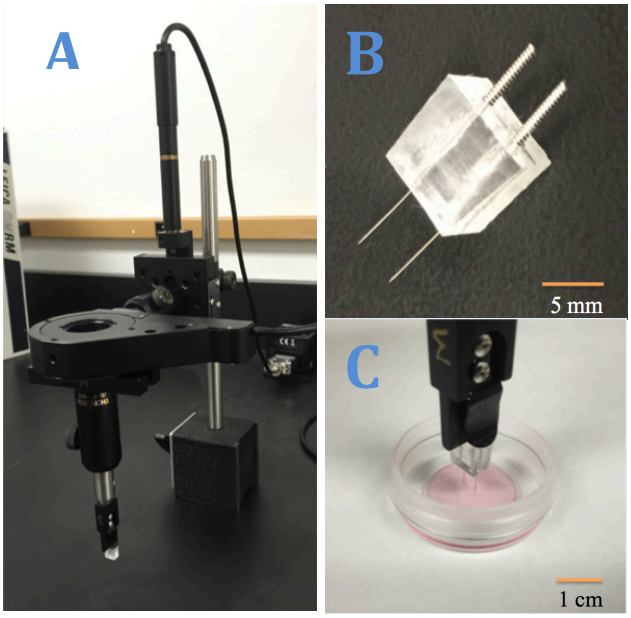

Figure 2: (A) The motor device used to generate rotational motion for alignment of collagen fibers. (B) PDMS block holding two needles used for collagen

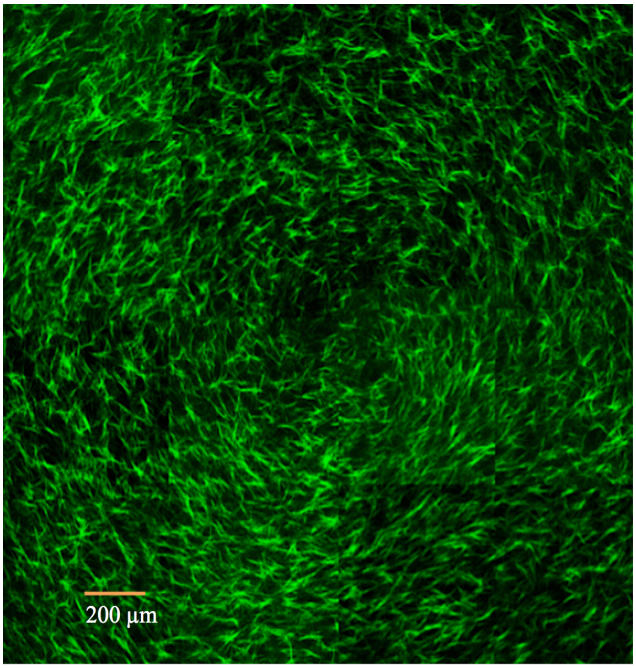

Figure 3: Image taken by a Leica Microsystems confocal microscope of circularly aligned collagen produced by stitching of a 4x4 grid of 16 images.

temperature for an additional 50 minutes for gelation to occur. The sample was then preserved in growth medium for 4-36 hours at 37 ˚C, after which the sample was stained and imaged for actin and vinculin.

Although the global alignment of collagen in the dish was circular, at a local level (in respect to the size of the cell) fiber alignment can be approximated to be linear. Cell samples were imaged and analyzed in the same fashion as the radially aligned samples.

CellTracker procedure:

For imaging, cells were labeled with CellTracker Red CMPTX Dye. The dye was diluted 1:1000 in PBS and applied to the sample after removal of growth media. It was allowed to incubate at 37˚C for 30 minutes, after which the diluted dye was removed, and replaced with growth media.

Vinculin staining procedure:

MDA-MB-231 cells were used for experimental purposes (including all staining and collagen procedures). Cell samples were fluorescently labeled with CellTracker Red before imaging (see CellTracker procedure). Growth media was removed from the sample and 1 mL of fixation solution (4% formaldehyde in PBS) was added and incubated at room temperature for 15 minutes. The sample was washed using PBS, and 1 mL of permeabilization solution (0.5% Triton X-

100 in DPBS) was added and allowed to incubate at room temperature for 15 minutes. The sample was then washed again using a PBS buffer, and 1 mL of blocking solution (3% BSA in DPBS) was added and allowed to incubate at room temperature for 1.5 hours. Blocking solution was then removed from the sample. 4 μL of the primary antibody (Vinculin Rb recombinant monoclonal Ab at stock concentration of 0.5 mg/mL) was diluted in 1 mL of blocking solution and added to the sample, which was incubated at 4 ˚C for approximately 36 hours. The sample was then washed with a PBS buffer.

4 μL of secondary fluorescent-labeled antibody (Alexa Fluor 647 goat anti-rabbit IgG (H+L) at stock concentration of 2 mg/mL) was diluted in 1 mL of PBS. The dye was then added to the sample and allowed to incubate for 2 hours at room temperature in the dark. The sample was then washed with a PBS buffer and preserved in PBS for imaging. The samples were stored in the refrigerator at 4 ˚C for further imaging and preservation.

Actin staining procedure:

Actin staining was carried out immediately after vinculin staining. Alexa Fluor 488 phalloidin dye was used for immunofluorescence labeling. Dye was stored in 1.5 mL ethanol as a stock solution. After completion of secondary antibody labeling for vinculin, the sample was washed with PBS. 25 μL of stock solution actin dye was diluted at a 1:40 ratio in PBS. 1% by volume of Bovine Serum Albumin was added to the dye solution. The diluted dye was added to the

sample and allowed to incubate at room temperature for 20 minutes. The sample was then washed in PBS and preserved in PBS for confocal imaging.

Confocal imaging procedure:

A Leica DMI400 B automated inverted microscope by Leica Microsystems was used for imaging of all samples. Two separate channels were used for imaging of cell body and collagen fibers.

For channel one (CellTracker fluorescence) a 532 nm laser was used for excitation and the detection range was set to 600 nm to 628 nm, and a DD 405/532 beamsplitter was used. For channel two (fiber reflections) a 532 nm laser was also used, and the detection wavelength was set to be 530 nm to 535 nm, and a RT 30/70 beamsplitter was used.

All images were taken using a 20X or 40 X oil objective. and Z-stacks were taken of individual cells for analysis. Each cell was centered on the XY-axis, and was sequentially imaged by progressing up the Z-axis from the bottom to the top of the cell. Step size was set to 0.5 μm. For analysis, one image was used from each Z-stack that displayed the maximum cell body cross-sectional area. Approximately 10-25 cells were imaged per sample. Frame average was set to 4 for noise suppression.

The same technique was used for imaging of actin and vinculin, using a 488 nm laser for excitation of fluorescently labeled actin, with a detection range

set to 500 to 535 nm. For vinculin imaging, a 635 nm laser was used with a detection range set to 640 to 700 nm. A TD 405/488/635 beamsplitter was used for both actin and vinculin channels. A 20X oil objective was used for all protein imaging.

Quantification of cell alignment:

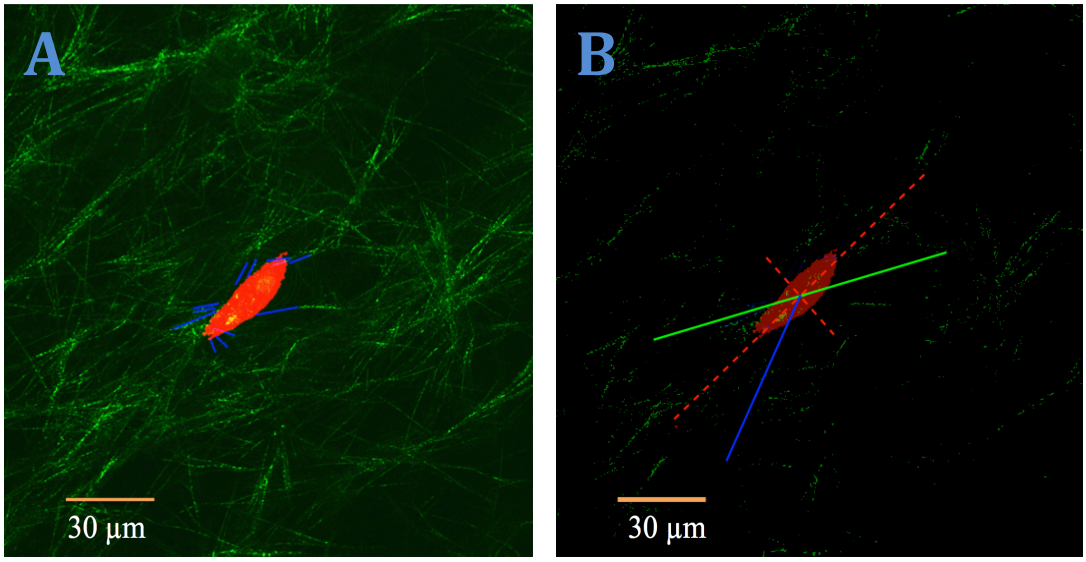

Figure 4: (A) Composite image of an MDA-MB-231 cell (red) and surrounding fibers (green). Blue lines indicate local fibers used to model and calculate average directionality of the local environment. (B) A quantitative image analysis of (A) showing the cell principle axes (red dotted lines), average local fiber alignment (blue), and collagen density gradient (green).

After imaging of the individual cells in the surrounding collagen matrix, a composite image was created for each cell (Fig 4A), with green representing collagen fibers, red as the maximum cross-sectional area of the cell, and blue as local fiber directionality. ImageJ was used to create a binary image of the maximum cross-sectional area of the cell body. The blue lines were added to indicate the spatial orientation of fibers immediately adjacent to the cell of

interest. These two images were combined with the green collagen channel to create the composite image shown (Fig 4A). Composite images produced were analyzed using MATLAB, measuring cell aspect ratio, average local fiber directionality, and cell directionality. A single representative image was given (Fig 4B). Approximately 200 cells were analyzed in this fashion.

RESULTS AND DISCUSSION

Influence of local environmental geometry on cell polarity:

Approximately 200 cells were imaged and analyzed. For each individual cell, aspect ratio of the maximum cross sectional area of the cell body was compared with the misalignment angle between average local fiber direction and cell alignment. The data collected showed a correlation between cell aspect ratio and the cell's alignment with average fiber direction (Fig 4), indicating that a mathematical relationship can be calculated between cell polarity and local environmental geometry. Using MATLAB, this data was found to be best modeled by a power law function of approximately $|\theta| = 40a^{-1.5}+6.7$, with a root mean square value of 15.9 (Fig 5). Additionally, MATLAB was used to model the relationship between $<\theta^2>$ and cell aspect ratio a, and was best modeled by a power law function of $<\theta^2> \sim a^{-1.9}$ (Fig 6).

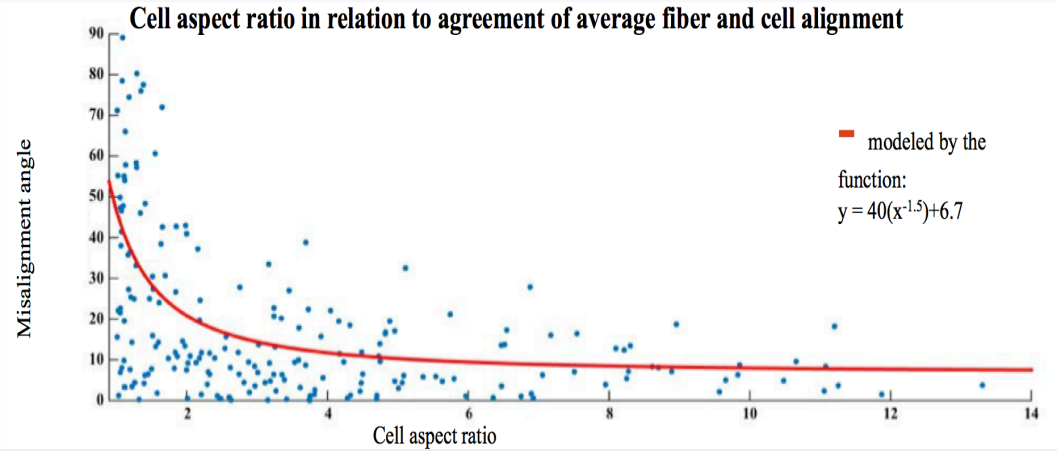

Figure 5: Cell aspect ratio is tightly correlated with the mismatch angle- the angle between the cell polarization and the extracellular fiber matrix. Non-linear curve fitting showing the data can be approximated by the function $y = 40(x^{-1.5})+6.7$ with an RMSE value of 15.9. A total of 200 data points were collected. Each data point represents one individual cell.

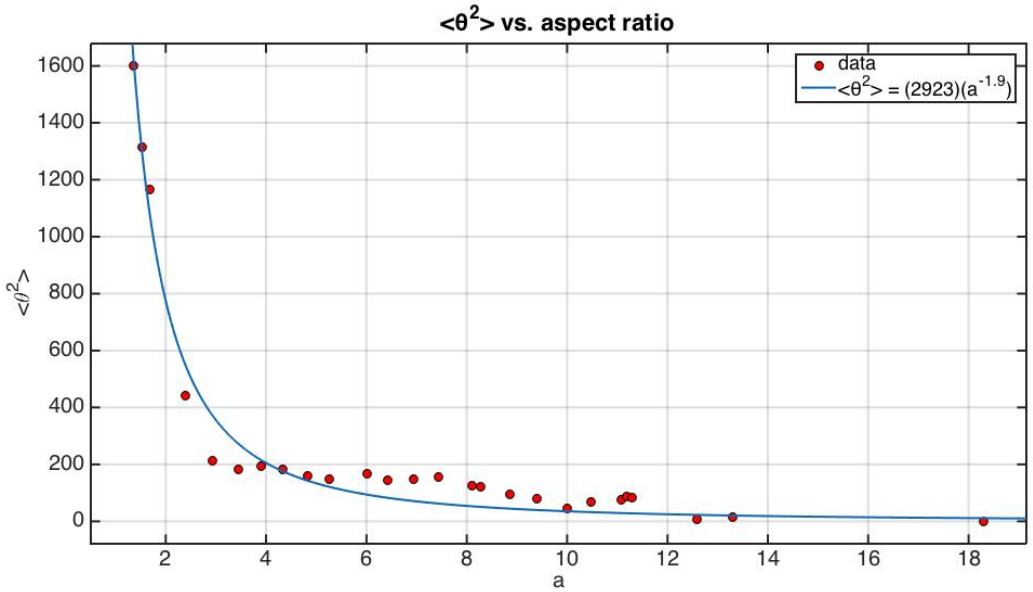

Figure 6: $< \theta^2 >$ calculated as a function of aspect ratio, best modeled by the power law function $< \theta^2 > = (2923)a^{-1.9}$. Coefficients were calculated with 95% confidence and a R-square value of 0.9768 was calculated. R-square value indicates the percentage of data (0-1.0) that can be explained by the curve fit, so a value of 0.9768 was deemed to be a good fit. All curve fitting was calculated using MATLAB.

As seen in figure 5, the non-linear data trend suggests a feedback system between cell morphogenesis and geometry of the respective microenvironment of the cell. In this feedback model, an organized fiber network triggers cellular alignment and elongation. The increased surface area resulting from cellular elongation would allow the cell to better contact and therefore align itself with the local fibers. As a result, a further decrease would be observed in the misalignment angle between the cell and average fiber direction. This feedback mechanism is proposed to give rise to the data trend observed, a relationship that is best modeled by a power law function. In summation, a linearly organized environment triggers cellular alignment, promoting the increase of cell aspect ratio and thereby allowing for even closer alignment with the fiber network. This

results in a non-linear relationship between cell morphogenesis and cell orientation with the geometry of the local microenvironment (in this case modeled by a spatially organized collagen fiber network).

Modeling ECM restoring force as a spring constant:

In order to better quantify this non-linear relationship, it has been modeled as a restoring spring force (Fig 7). Assuming θ takes Guassian distribution (Eq. 1):

$$P(\theta) \sim e^{\wedge}(-\theta^2/2\sigma^2) \qquad \text{(Eq. 1)}$$

which is a result of random intrinsic noise from the cell confined by a spring of strength k. Therefore, we have

$$\langle\theta^2\rangle \sim \sigma^2 \sim 1/k \qquad \text{(Eq. 2)}$$

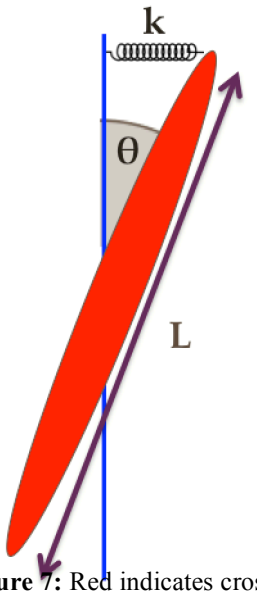

Figure 7: Red indicates cross-sectional area of cell body and blue line represents local fiber directionality. L = cell major axis length, k = spring force, θ = misalignment angle.

Assuming cell volume V = 2π/3 L (L/a)^2 is conserved during its elongation, cell aspect ratio a and cell length L are related as

$$a \sim L^{1.5} \qquad \text{(Eq. 3)}$$

From the data gathered, we found $\langle\theta^2\rangle \sim a^{-1.9}$, therefore, the spring constant k can be scaled as the length of the major cell axis to a power of 2.9 (Eq. 4).

$$k \sim L^{2.9} \qquad \text{(Eq. 4)}$$

This is inconsistent with the expectation that harmonic springs are uniformly distributed along the cell major axis, in which case we would have k ~ L. Therefore, one has to incorporate non-linear effects such as aharmonic springs, or self-induced aggregations of springs along the cell. To further distinguish these possible scenarios, we will need a better understanding of the microscopic mechanisms involved. To this end, we turn to immunofluorescent studies of key molecular players.

Vinculin and actin staining in 3D:

Both actin and vinculin have been shown to be crucial proteins involved in cell mechanosensing[7]. Staining of vinculin and actin molecules in cells embedded in a three-dimensional collagen matrix (same conditions were used for protein staining as in analysis of cell morphology and environmental geometry) revealed spatial organization of these proteins as well, signified by the tendency for actin filaments to orient along the same axis as the respective cell and were observed to be especially organized in elongated cells (Fig 8). Vinculin was often observed to be present at higher densities around outer edges of the cell, concurrent with its role in focal adhesion functionality. These observations are also consistent with the spatial organization of vinculin and actin observed in mechanosensing in two dimensions, indicating similar mechanisms of polarization in both mechanosensing and geometry sensing.

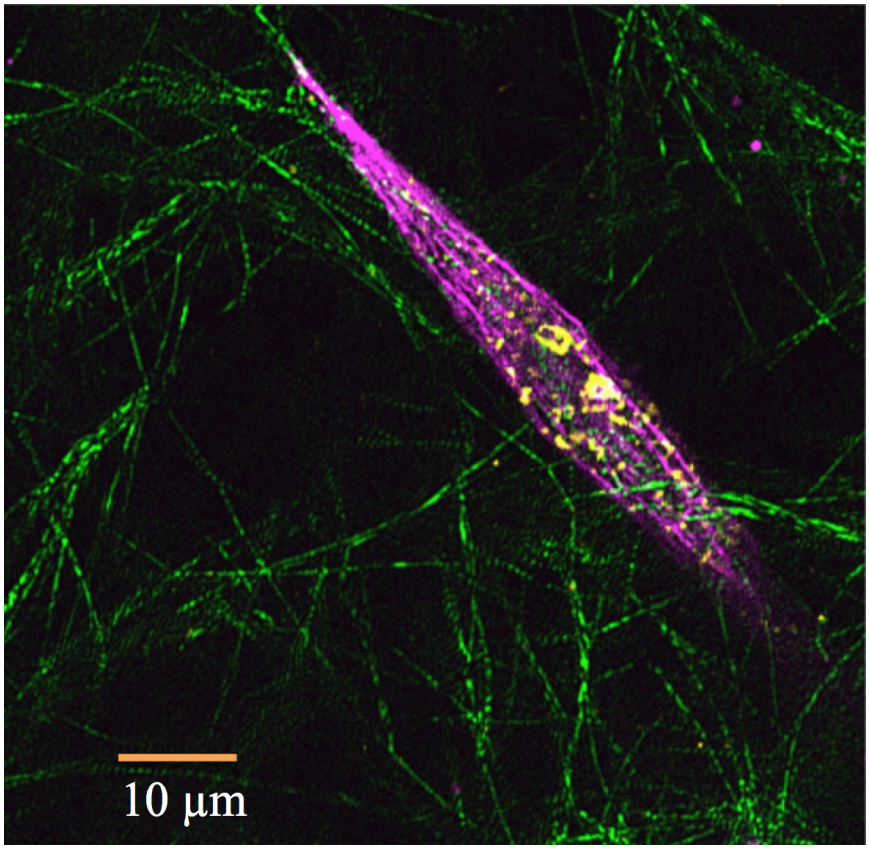

Figure 8: The cytoskeleton of a MDA-MB-231 cell integrated with the extracellular collagen fiber network. The sample was immunostained for actin (purple) and vinculin (yellow) in collagen matrix (green).

Conclusions and future applications:

The use of contact guidance as a tool for the development of highly organized tissue could prove to be very useful in the future of tissue engineering and is already a cellular mechanism employed in living organisms. Mouse cerebral granule cells have been shown to exhibit contact guidance along neurites, a process that is essential for proper nervous system development[8]. In addition, higher alignment of collagen is correlated with an increased rate of poor outcome in breast cancer patients. Stromal collagen in breast tissue tends to have a dense,

highly aligned matrix, and it is observed that an increase in the level of fiber alignment appears to promote migration along the fiber directionality thus enhancing the growth and metastasis of the cancer tissue[9]. Contact guidance has also been previously utilized in the field of bioengineering to test the benefit of implanting pre-vascularized networks to improve host acceptance and growth of donor tissues[10].

For these reasons, the manipulation of contact guidance to direct cell morphology and growth in three-dimensions (and ultimately tissue growth) is especially applicable in bioengineering and cancer metastasis research. However, the cellular mechanisms behind geometry sensing have not been researched to the same extend as other cellular sensing processes such as chemosensing. This is especially true for geometry sensing in a three-dimensional environment.

To better our understanding of cell geometry sensing in three dimensions, the objective of this project was to mathematically quantify the relationship between breast cancer cell morphogenesis and the geometry of the cell's microenvironment, as modeled by a spatially organized collagen matrix. A correlation was observed between cell morphology and cell alignment with the average direction of the local fiber network. This relationship was modeled by a power law function with "y" representing the misalignment angle between cell and average fiber direction and "x" representing cell aspect ratio. This was calculated as $y = 40(x^{-1.5})+6.7$ with an RMSE value of 15.9. The non-linear mathematical nature of this relationship is indicative of a feedback system between cell morphogenesis and cell alignment with the geometry of the local

microenvironment. To assess the properties of geometry sensing at a molecular level, confocal immunofluorescent imaging was used to compare the spatial organization of actin and vinculin known to be present in mechanosensing to that in three-dimensional geometry sensing. The linear polymerization of actin filaments and presence of vinculin clusters observed in cells exhibiting contact guidance were qualitatively similar to the presence of these proteins in mechanosensing. This suggests a possible similarity in the cellular mechanisms behind geometry sensing and mechanosensing. My assessment of cellular response in a three-dimensional matrix on a morphological and molecular level begins to provide some insight to the knowledge gap regarding the characteristics of contact guidance.

Sources cited

1.) E. Vrana, N. Builles, M. Hindie, O. Damour, A. Aydinli, V. Hasirci. Contact guidance enhances the quality of a tissue engineered corneal stroma. *Journal of Biomedical Materials Research* 84.2 (2008): 454-463.

2.) Etienne-Manneville, Sandrine; Alan Hall. Integrin-Mediated Activation of Cdc42 Controls Cell Polarity in Migrating Astrocytes through PKCζ. *Cell*. 106.4 (2001): 489-498.

3.) Vicente-Manzanares, Miguel; Donna J. Webb, A. Rick Horwitz. Cell migration at a glance. *Journal of Cell Science*. 118 (2005): 4917-4919.

4.) Beningo, Karen A., Micah Dembo, Yu-li Wang. Responses of fibroblasts to anchorage of dorsal extracellular matrix receptors. *Proceedings of the National Academy of Sciences* 101.52 (2004): 18024-18029.

5.) Teixeira, Ana I.; George A. Abrams, Paul J. Bertics, Christopher J. Murphy, and Paul F. Nealey. Epithelial contact guidance on well-defined micro- and nanostructured substrates. *Journal of Cell Science.* (2003): 116 1881-1892.

6.) Friedl, Peter, Kerstin Maaser, C. Eberhard Klein, Bernd Niggemann, Georg Krohne, and Kurt S. Zanker. Migration of Highly Aggressive MV3 Melanoma Cells in 3-Dimensional Collagen Lattices Results in Local Matrix Reorganization and Shedding of a2 and B1 Integrins and CD44. *Cancer Research* 57 (1997): 2061-2070.

7.) Michael E. Ottlinger; Lin, Shin. *Clostridium difficile* toxin B induces reorganization of actin, vinculin, and talin in cultured cells. *Experimental Cell Research*. 174.1 (1988): 215-229.

8.) Nagata I., Nakatsuji N. Rodent CNS neuroblasts exhibit both perpendicular and parallel contact guidance on the aligned parallel neurite bundle. *Development*. 112 (1991): 581–590

9.) Riching, Kristin M., et al. 3D Collagen Alignment Limits Protrusions to Enhance Breast Cancer Cell Persistence. *Biophysical Journal.* 107 (2014): 2546-2558.

10.) Baranskia, Jan D., Chaturvedia, Ritika R.; Kelly R. Stevensb, Jeroen Eyckmansa, Ricardo D. Solorzanoa, Brian Carvalhob, Michael T. Yanga, Jordan S. Millera, Sangeeta N. Bhatiab, Christopher S. Chena. Geometric control of vascular networks to enhance engineered tissue integration and function. *Proceedings of the National Academy of Sciences of the United States of America.* 110.19 (2013): 7586-7591.

11.) Provenzano, Pablo P.; Kevin W. Eliceiri, Jay M. Campbell, David R. Inman, John G. White, Patricia J. Keely. Collagen reorganization at the tumor-stromal interface facilitates local invasion. *BMC Med.* (2006): 4:38

12.) Carisey A, Tsang R, Greiner AM, et al. Vinculin Regulates the Recruitment and Release of Core Focal Adhesion Proteins in a Force-Dependent Manner.*Current Biology*. 2013;23(4):271-281.